

# **RADIOLOGICAL CHARACTERIZATION OF THE ACTIVATION OF THE STRUCTURE MATERIALS OF THE BR1 RESEARCH REACTOR**

Nadia Messaoudi, Hamid Aït Abderrahim, Luc Noynaert  
SCK•CEN, Boeretang 200 B-2400 Mol, Belgium  
[nmessaou@sckcen.be](mailto:nmessaou@sckcen.be)

## **ABSTRACT**

This paper presents a radiological characterization of structure materials of the BR1 research reactor. BR1 is a natural uranium fuelled, graphite moderated and gas (air) cooled reactor. The objectives of this study are (1) to predict the type and the quantity of activation products (isotope-by-isotope) formed over the operating life of the reactor BR1 and remaining after a given cooling time and (2) to evaluate the structure materials activation ( $\alpha$ ,  $\beta$  or  $\gamma$  activations) at different time scales after the definitive predicted shutdown of the reactor.

For this purpose, a calculation methodology was defined: The SCALE4.3 code system, in conjunction with the 238 neutron group library (based on ENDF/B-V data file) was used to generate cross section for all relevant materials. For the 2-dimensional spatial flux determination, the neutron transport code DORT was used. From the 2-D flux map, activations are obtained by using the ORIGEN2 code and taking into account the detailed operational history.

This work concerns both the graphite (reflector) and the concrete (biological shielding) of the BR1 reactor. Main results are as follows: we notice that in the concrete and the graphite, the flux is almost thermal (more than 90% of total flux has energy below 0.5 eV), so this enhances the thermal activation reactions such as  $^{40}\text{Ca}(n, \gamma)^{41}\text{Ca}$ ,  $^{54}\text{Fe}(n, \gamma)^{55}\text{Fe}$ , etc. For the graphite zone,  $^{14}\text{C}$  remains the dominating participant to the activity after 5 years of cooling time. There is also production of other activation products such as  $^{55}\text{Fe}$  and  $^{63}\text{Ni}$ . In graphite, we underline the generation of  $^{60}\text{Co}$  formed by capture reaction on Fe and Ni (Fe and Ni are initially present in graphite as impurities),  $^{60}\text{Co}$  is a high energy gamma emitter. For concrete,  $^{133}\text{Ba}$  is by far the principal producer of activity but we underline also  $^{55}\text{Fe}$  and  $^{41}\text{Ca}$  contributions:  $^{55}\text{Fe}$  is the most active during the first years of cooling time and the  $^{41}\text{Ca}$  contribution becomes more significant after a long term scale. In concrete, the specific activity is strongly spatially dependent.

## **1. INTRODUCTION**

BR1, the 4-MW first research reactor built in Belgium, is currently operated at 700 kW on daily regime. Its shutdown is planned for 2020. So, before its dismantling, it is of primary

importance to assess the types and quantities of waste generated by contamination or activation of the BR1 structure materials under irradiation and after cooling time.

In the framework of the radiological characterization of structure materials of BR1, the main aims of the present study are to establish a calculation methodology for activation study (codes, nuclear data), to identify activation products generated under irradiation in graphite B (reflector) and concrete (shielding material), to distinguish which of them remain after different cooling times and to establish the maximum level of activity in the various zones of BR1.

Section 2 gives a brief description of the BR1 reactor (reactor geometry and structure materials compositions). In Section 3, the calculation methodology and computer codes used in the study are presented. The main results and discussions are summarized in Section 4. Finally, the conclusions are given in Section 5.

## 2. DESCRIPTION OF THE BR1 REACTOR

BR1 is the first Belgian research reactor [1]. It is in operation at SCK•CEN since 1956. The maximum nominal power is 4 MW but, at the present time, it is operated at 700 kW thermal power on an 8 hours daily basis. BR1 is a natural uranium fuelled, graphite moderated and gas (air) cooled reactor. A particularity of BR1 is that it consists of a large core. The core zone is a stack of 14500 graphite blocks with a volume as follows: 6.66 m (length)  $\times$  6.84 m (width)  $\times$  6.84 m (height). 829 channels, with square section  $5 \times 5 \text{ cm}^2$ , are passing through these blocks. Only 569 of these channels are loaded with fuel. There are 23 fuel elements in each channel. A fuel element consists of a cylindrical bar with aluminum cladding: its outer dimensions are 20.3 cm length and 2.54 cm diameter.

In the BR1 core, there are two kinds of graphite, depending on their different compositions and functions [2]:

- graphite A, in the central zone ( $R < 2.62 \text{ m}$ ) of the core; its density is  $1.62 \text{ g/cm}^3$  and it contains 0.4 ppm of boron: this is the moderator.
- graphite B, beyond 2.62 m from the core center; its density is  $1.72 \text{ g/cm}^3$  and it contains 1.6 ppm of boron, it is used as reflector; this graphite contains some impurities such as Fe, Al, K, Ca, Ni and V (See Table I).

The core is surrounded by concrete of 2.10 m in thickness, which serves as a biological shielding (See Figure 1). The concrete of BR1 is a heavy barite concrete with a density of  $3.4 \text{ g/cm}^3$ . It contains an important amount of barium representing more than 45% weight percent, other elements such as Fe, Ca, etc. are also present in this concrete. They are important from the point of view of activation (See Table II).

## 3. METHODOLOGY AND CODES

The nuclear data needed for neutron activation studies fall into two categories:

1. multigroup neutron cross sections for use in transport calculations to compute the space and the energy dependent neutron fluxes, and

2. activation cross sections and decay data for all important parent and daughter isotopes that can be generated via neutron activation under irradiation or after the cooling time.

Figure 2 illustrates the whole calculation procedure. First, a cell calculation was performed using the code system SCALE version 4.4 [3]. Mainly the modules BONAMI, NITAWL, XSDRNPM and ICE were used to generate mixed macroscopic cross sections for all relevant materials of BR1. The cross section library utilized is the '238groupndf5' library with 148 fast groups and 90 thermal ones based on ENDF/B-V.

Secondly, to take into account the spatial spectrum dependency in the core and to collapse the generated 238 group cross sections to 27 group ones, a 1-D transport calculation using the module XSDRNPM was carried out for a one-dimensional modeling of the whole core. This calculation produced a 27 group region wise cross section data set for core calculations.

Thirdly, the core calculation was performed using the 2-D transport code DORT (version 3.1) [4] to derive the spatial flux map in the graphite and the concrete zones. In fact, because of the huge size of the BR1 reactor, core calculations were carried out in two steps: first, a criticality calculation ( $k_{\text{eff}}$ ) that gives the spatial flux distribution in the graphite and also the spatial source distribution in the core, secondly, the source distribution was used in a fixed source calculation to obtain the flux map in the concrete. BR1 was modeled in (X, Y) geometry and a buckling correction was applied to take into account the axial neutron leakage for the  $k_{\text{eff}}$  calculation.

Finally, activation calculations were carried out with the zero-dimensional code ORIGEN2 [5] in conjunction with the detailed operational history of BR1 [2]. The evolution of the nuclide concentrations and activities were calculated in ORIGEN2 using one group cross sections, stored in libraries obtained by averaging neutron-energy-dependent cross sections over the typical reactor neutron energy spectra. For this study, the 2200 m/s cross section library was used. The reason is explained in Section 4. The 2200 m/s flux used is defined as follows:

$$\phi_{\text{thermal}} = v_0 \times \int_0^{0.5\text{eV}} n(E) \times dE$$

where  $v_0 = 2200$  m/s, the neutron speed corresponding to the neutron energy of 0.025 eV, and  $n(E) dE$  number of neutrons with energy E in the interval dE.

The irradiation history of BR1 is complicated and variable. Since 1957, when BR1 started to operate, there were two modes of operation: the first one consisted of long irradiation cycles of 2 or 3 weeks followed by about one week as cooling period at the nominal power of 4 MW. This mode took end in 1964. The second mode is a daily short cycle: 8 hours of irradiation per day at the nominal power of 700 kW.

For this study, the irradiation history was simplified by converting it into a series of continuous irradiation periods of 1 year followed by a cumulated and appropriate cooling time for each mode [2].

Initial isotopic composition of fuel (i. e., fresh fuel) was used for cell and core calculations; a preliminary calculation concerning fuel composition evolution with respect to the operational

history and power was undertaken [2]. The result showed that the composition of the fissile isotope  $^{235}\text{U}$  does not change significantly: the variation reached after more than 40 years of irradiation is about 5%. This is due to the low level of the BR1 power and its irradiation history (See the preceding paragraph).

In addition, the graphite in the BR1 reactor is assumed to be a natural carbon (abundances of  $^{12}\text{C}$  and  $^{13}\text{C}$  are 98.9 and 1.10 respectively) [6].

## 4. RESULTS AND DISCUSSIONS

The activations of both graphite B and concrete of BR1 were evaluated at the end of irradiation and after different cooling times: 5 and 10 years (sometimes, to get more detailed information, we extended the cooling time to 15 or 20 years). Specific activity calculations were carried out with the ORIGEN2 code with the 2200 m/s cross section library instead of generating our own cross sections for the activation calculation. This choice is justified by the fact that the spectrum in the graphite B and concrete zones is fully thermal: the majority of the neutronic population is located at energies below 0.5 eV (See Figures 3 and 4). This enhances the thermal activation reactions.

In this paper, the results concerning the activation calculation will be given for both graphite B (the BR1 reflector) and concrete at some positions in the mid-plane, where we expect to reach the maximum values of activation. The activation of graphite A (the BR1 moderator) is not treated in the present paper.

### 4.1 GRAPHITE B

Figure 5 shows that, in the graphite B zone, the total flux in the mid-plane varies between  $1.53 \cdot 10^{11}$  n/cm<sup>2</sup>.s (at the entry in this region) and  $2.63 \cdot 10^{09}$  n/cm<sup>2</sup>.s (just before the air zone). The specific activity is calculated for these two points in order to have an overview of the activity variation according to the graphite B distance from the core center. Specific activities coming from the main activation products in graphite B are summarized in Table III.

The activity in the graphite B is mainly due to the activation products:  $^{14}\text{C}$ ,  $^{55}\text{Fe}$  and  $^{63}\text{Ni}$ . In fact,  $^{14}\text{C}$ , which is generated by neutronic capture reaction  $^{13}\text{C}(n, \gamma)^{14}\text{C}$ , is the major contributor to the activity at different time scales. After 10 years of cooling time, its contribution reaches 92.6% of the total activity:  $^{14}\text{C}$  is a long-lived activation product ( $T_{1/2}=5715$  years) compared to  $^{55}\text{Fe}$  ( $T_{1/2}=2.73$  years) and generated in significant amount compared to  $^{63}\text{Ni}$  ( $T_{1/2}=100$  years). On the long-term scale, the total activity is completely dominated by the  $^{14}\text{C}$  contribution which emits  $\beta^-$  particles at 157 keV.

The amount of trace elements in graphite B, such as Fe and Ni, has an influence (but slightly) on the resulting activation.  $^{55}\text{Fe}$  and  $^{63}\text{Ni}$  are formed by capture reaction (n,  $\gamma$ ) on  $^{54}\text{Fe}$  and  $^{62}\text{Ni}$  respectively, they are the most active contributors after  $^{14}\text{C}$ . The  $^{55}\text{Fe}$  contribution to the total activity decreases from 22.27% at the end of the irradiation to 1.97% after 10 years of cooling time, while the  $^{63}\text{Ni}$  contribution remains almost constant (~5%) at different time scales.

The presence of  $^{58}\text{Fe}$  in graphite leads to  $^{60}\text{Co}$  generation under irradiation ( $^{58}\text{Fe}(n, \gamma) ^{59}\text{Fe}$ ,  $^{59}\text{Fe} (\beta^-)^{59}\text{Co}$  and  $^{59}\text{Co} (n, \gamma)^{60}\text{Co}$ ). This product is a gamma emitter with high energies: 1.3325 MeV and 1.1732 MeV.

Others activation products such as  $^{40}\text{K}$ ,  $^{41}\text{Ca}$ , and  $^{59}\text{Ni}$  are also generated, they are formed mainly by capture reaction on  $^{39}\text{K}$ ,  $^{40}\text{Ca}$ , and  $^{58}\text{Ni}$  but without significant contribution to the total activity. The thermal capture cross section of  $^{40}\text{Ca}$  is not very large (0.41 barns) whereas the capture cross section of  $^{58}\text{Ni}$  is 4.6 barns, but the initial amount of  $^{58}\text{Ni}$  present in graphite is low [6].

We notice that the specific activity is spatially dependent. Figure 6 gives an overview of the activity variation as a function of the distance in the graphite B zone. For instance, after 10 years of cooling time, the specific activity drops from 243 Bq/g for the highest flux position to 4.66 Bq/g for the lowest flux position.

#### 4.2 IMPACT OF COBALT (Co) OR EUROPIUM (Eu) IMPURITIES

As we notice (See Table I), the initial composition of BR1 graphite does not contain any trace of either Co or Eu, but these are commonly present as impurities in graphite and are of importance from the point of view of the total activity they induce. Their activation products are  $\gamma$  emitters with high energies. So, it is interesting to estimate the potential impact of these elements on the activity of BR1 graphite.

In this study, we treat the impact of each element individually and assume that traces of Co and Eu are present, namely 0.01 ppm and 0.001 ppm respectively. These values are usually present as impurities in graphite and considered in calculations [7].

Table IV shows that 0.01 ppm of Co increases slightly the total activity (only 1.15 times) after irradiation at the highest flux. In fact, the situation is mainly dominated by  $^{14}\text{C}$  contribution (more than 60% at the end of irradiation). The Co contribution to the total activity in the first years after the shutdown is between 13% and 9% (See Figure 7). After 5 years, this contribution decreases and the total activity is almost similar to the reference case (graphite B without impurities).  $^{60}\text{Co}$  ( $T_{1/2}=5.271$  y) decays by emission of  $\gamma$  radiations at high energies 1.3325 MeV and 1.1732 MeV.  $^{60}\text{Co}$  is produced almost entirely by thermal and epithermal neutron capture in  $^{59}\text{Co}$  (in our case, there is only a thermal contribution).

Concerning the impact of 0.001 ppm of Eu, we notice (See Table IV) that the total activity is increased significantly by  $^{152}\text{Eu}$  and  $^{154}\text{Eu}$  contributions but  $^{14}\text{C}$  remains the dominant contributor for different time scales.  $^{152}\text{Eu}$  contributes to the total activity by 20% on a time scale of 5 to 10 years. This isotope is produced primarily by thermal neutrons (See Figure 8).

We can conclude that the presence of impurities such as Co or Eu in graphite B does not affect the total activity if we consider a long cooling time because  $^{14}\text{C}$  becomes the main contributor due to its long half-life. But one has to be aware of the fact that their activation products emit  $\gamma$  radiations at high energies even if they are generated in insignificant amount.

#### 4.3 CONCRETE

As shown in Figure 1, the zone A in the concrete is the most close to the core and consequently the most exposed to the high neutron flux escaping from the core region.

Therefore, we expected that this zone would be the most activated. In this section, the activation in this zone A is therefore evaluated: more exactly some positions on the diagonal ( $\psi=45^\circ$ ) are selected, they are located at 12.5 cm from each other, reference position (0 cm) is the entry in the concrete.

The main results concerning the concrete characterization are summarized in Table V. At the entry in the concrete (at  $\psi=45^\circ$ ), the flux is relatively high about  $2.25 \cdot 10^9$  n/cm<sup>2</sup>.s (compared to the flux at the core center  $2.51 \cdot 10^{11}$  n/cm<sup>2</sup>.s).

Figure 9 shows that the flux in the concrete is strongly spatially dependant, for instance, at 75 cm from the surface of the concrete wall, the flux is reduced by a factor of  $4.0 \cdot 10^7$ . The spectrum is completely thermal; this enhances activation reactions induced by thermal neutrons (See Figure 4).

BR1 concrete contains a significant amount of barium (45% weight percent), plus other elements such as S, Si, Ca, O, Fe, Al, Hg, H, B and Mg.

For the reference point (at the entry in the concrete), the specific activity, induced by the high flux ( $2.25 \cdot 10^9$  n/cm<sup>2</sup> s) reaches  $2.50 \cdot 10^4$  Bq/g at the end of irradiation and decreases to  $5.28 \cdot 10^3$  Bq/g after 10 years of cooling time. In fact, at the end of irradiation, the activity is mostly dominated by the contribution of <sup>55</sup>Fe (55.5%) and <sup>133</sup>Ba (31.6%).

<sup>55</sup>Fe is formed by capture reaction on <sup>54</sup>Fe (present initially in concrete with weight percent 4.41%). The <sup>55</sup>Fe contribution decreases to about 18.3% after 10 years cooling time whereas <sup>133</sup>Ba becomes the major contributor to the total activity (78%). Normally, <sup>133</sup>Ba is generated by both thermal and epithermal capture reaction on <sup>132</sup>Ba [8]. In our case, the spectrum in concrete is completely thermal, so, the epithermal contribution is not taken into account (See Figure 10). The thermal capture cross section of <sup>132</sup>Ba is low (0.8 barns) [6]. Nevertheless, the fact that the BR1 concrete contains a large quantity of barium allows a significant <sup>133</sup>Ba production and consequently an important activity contribution. <sup>133</sup>Ba emits a series of relatively low energy gammas, at 0.365, 0.3029 and 0.081 MeV.

Besides <sup>55</sup>Fe and <sup>133</sup>Ba which are the major contributors to total activity in the concrete zone, there are other activation products:

1. <sup>41</sup>Ca is produced entirely by thermal capture on <sup>40</sup>Ca (96.94% abundant), its neutron capture section is not large (0.41 barns), but on the long term scale, the <sup>41</sup>Ca contribution increases because of its long half-life ( $T_{1/2}=1.03 \cdot 10^{05}$  years).
2. Traces of <sup>36</sup>Cl, <sup>10</sup>Be, <sup>14</sup>C, <sup>45</sup>Ca but with insignificant activity contributions.

In summary, the activity level in the concrete zone is strongly spatially dependent and hence the neutron energy spectrum and flux values and the composition of the concrete play a major role in the activity level.

## 5. CONCLUSIONS

This paper presents the calculation methodology used for the activation evaluation of the BR1 structure materials (graphite B and concrete), namely codes: SCALE, DORT and ORIGEN2 and nuclear data: '238groupndf5' based on ENDF/B-V. The main aims of this study were on

the one hand to establish the maximum limit of the activation produced and on the other hand to identify the major contributors to the activity at different time scales.

The results show that (1) the spectrum is completely thermal in these areas, which is advantageous for thermal activation reactions and (2) the activity is spatially dependent for both zones but more strongly in concrete where it drops rapidly in the concrete because of the flux depression.

For the graphite zone,  $^{14}\text{C}$  remains the dominating participant to the activity after 5 years of cooling time, even in presence of impurities such as Co or Eu. Besides  $^{14}\text{C}$  production, other activation products such as  $^{55}\text{Fe}$  and  $^{63}\text{Ni}$  are generated but they are less important in terms of contribution. In the graphite, we underline also the generation of  $^{60}\text{Co}$  formed by capture reactions on Fe and Ni (Fe and Ni are initially present in graphite),  $^{60}\text{Co}$  is a high energy gamma emitter.

In the concrete zone, the flux values and hence the activity level are strongly spatially dependent. As contributor to the activity,  $^{133}\text{Ba}$  is by far the principal producer of activity but we underline also  $^{55}\text{Fe}$  and  $^{41}\text{Ca}$  contributions,  $^{55}\text{Fe}$  is the most active during the first years of cooling time and the  $^{41}\text{Ca}$  contribution becomes more significant after a long term scale.

## REFERENCES

1. "Réacteur BR1: Rapport de sûreté destiné au renouvellement des autorisations du CEN/SCK" SCK•CEN report, December 1985.
2. N. Messaoudi, "Caractéristiques du BR1 et Etude de l'Aspect Temporel du BR1" SCK•CEN report, to be published in 2000.
3. C. V. Parks, *et al.*, "SCALE-4: An Update Version of the Modular Code System for Performing Standardized Computer Analysis for Licensing Evaluation," Proceedings of ANS/ENS: International Topical Meeting on Advances in Mathematics, Computations and Reactors Physics, Pittsburgh, USA, (1991).
4. W. A. Rhoades and R. L. Childs, "The DORT Two-Dimensional Discrete Ordinates Transport Code", *Nuclear Science and Engineering*, **99**, pp. 88-99, (May 1998).
5. A. G. Croff, "ORIGEN2: A Versatile Computer Code for Calculating the Nuclide Compositions and Characteristics of Nuclear Materials". *Nuclear Technology*, **62**, pp. 335-352 (1983).
6. W. Walker, *et al.*, "Chart of the Nuclides", Fifteenth Edition, General Electric Company, 1996.
7. "Destruction by Incineration of the Moderator Graphite of U. N. G. G. Reactors, Dismantling", French Atomic Energy Commission (CEA) report, PNL-TR-455, December 1978.
8. J. C. Evans, *et al.*, "Long Lived Activation Products in Reactor Materials", Pacific Northwest Laboratory report, NUREG/CR-3414, August 1984.

Table I. Impurities in Graphite B

Isotopes	Impurities (ppm)
B	1.60
Fe	4.39
Al	29.65
K	9.82
Ca	0.63
Ni	0.14
V	1.60

Table II. Composition of BR1 Concrete (density = 3.4 g/cm<sup>3</sup>)

Element	Weight percent (%)
Ba	45.5882
O	31.1765
S	10.5882
Ca	4.7059
Si	1.7647
Fe	4.4118
Al	0.5882
H	0.6471
Mg	0.2059
B	0.0235

Table III. Specific activity due to the maximum flux in Graphite B

Activation products	Specific activity (Bq/g-graphite B)		
	End of irradi.	+ 5 years	+10 years
<sup>10</sup> Be	4.64E-03	4.64E-03	4.64E-03
<sup>14</sup> C	2.25E+02	2.25E+02	2.25E+02
<sup>36</sup> Cl	5.23E-03	5.23E-03	5.23E-03
<sup>39</sup> Ar	1.18E-10	1.18E-10	1.18E-10
<sup>40</sup> K	8.68E-04	8.68E-04	8.68E-04
<sup>41</sup> Ca	1.17E-01	1.17E-01	1.17E-01
<sup>45</sup> Ca	1.22E+00	5.15E-04	2.18E-07
<sup>50</sup> V	2.58E-11	2.58E-11	2.58E-11
<sup>55</sup> Fe	6.89E+01	1.82E+01	4.79E+00
<sup>60</sup> Co	8.04E-03	4.17E-03	2.16E-03
<sup>59</sup> Ni	1.43E-01	1.43E-01	1.43E-01
<sup>63</sup> Ni	1.40E+01	1.35E+01	1.30E+01
<sup>65</sup> Zn	4.45E-09	1.06E-09	1.36E-09
Total	3.09E+02	2.57E+02	2.43E+02

Table IV. Comparison of total activities due to maximum and minimum flux in Graphite B of BR1

		Flux (n/cm <sup>2</sup> s)	Specific activity (Bq/g)		
			End of irradiat.	+ 5 years	+10 years
Max. flux	Graphite B	1.53E+11	3.09E+02	2.57E+02	2.43E+02
	Graphite B + 0.01 ppm Co	1.53E+11	3.55E+02	2.81E+02	2.55E+02
	Graphite B + 0.001 ppm Eu	1.53E+11	4.30E+02	3.46E+02	3.11E+02
Min. flux	Graphite B	2.63E+09	5.95	4.93	4.66
	Graphite B + 0.01 ppm Co	2.63E+09	6.83	5.39	4.90
	Graphite B + 0.001 ppm Eu	2.63E+09	1.07E+01	8.57	7.46

Table V. Specific activity and flux in the BR1 concrete vs. distance

Distance (cm)	Flux (n/cm <sup>2</sup> s)	Specific activity (Bq/g)		
		End of irradiat.	+ 5 years	+10 years
0: entry in concrete	2.25E+09	2.50E+04	9.55E+03	5.28E+03
12.5	6.46E+07	7.19E+02	2.75E+02	1.52E+02
25	1.47E+06	1.63E+01	6.25E+00	3.46E+00
37.5	3.22E+04	3.58E-01	1.37E-01	7.57E-02
50	1.76E+03	4.68E-02	2.75E-02	1.89E-02
62.5	2.43E+02	2.70E-03	1.03E-03	5.70E-04
75	5.64E+01	6.27E-04	2.40E-04	1.33E-04

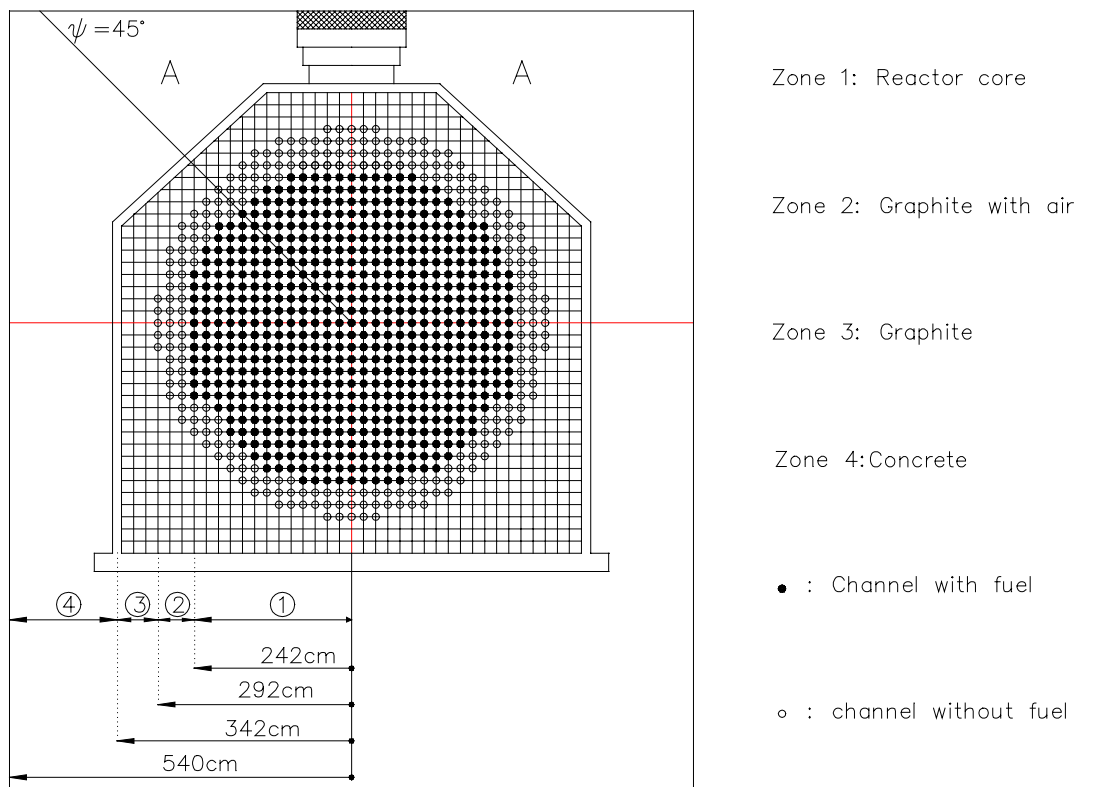


Figure 1. Axial schematic view of the BR1 reactor

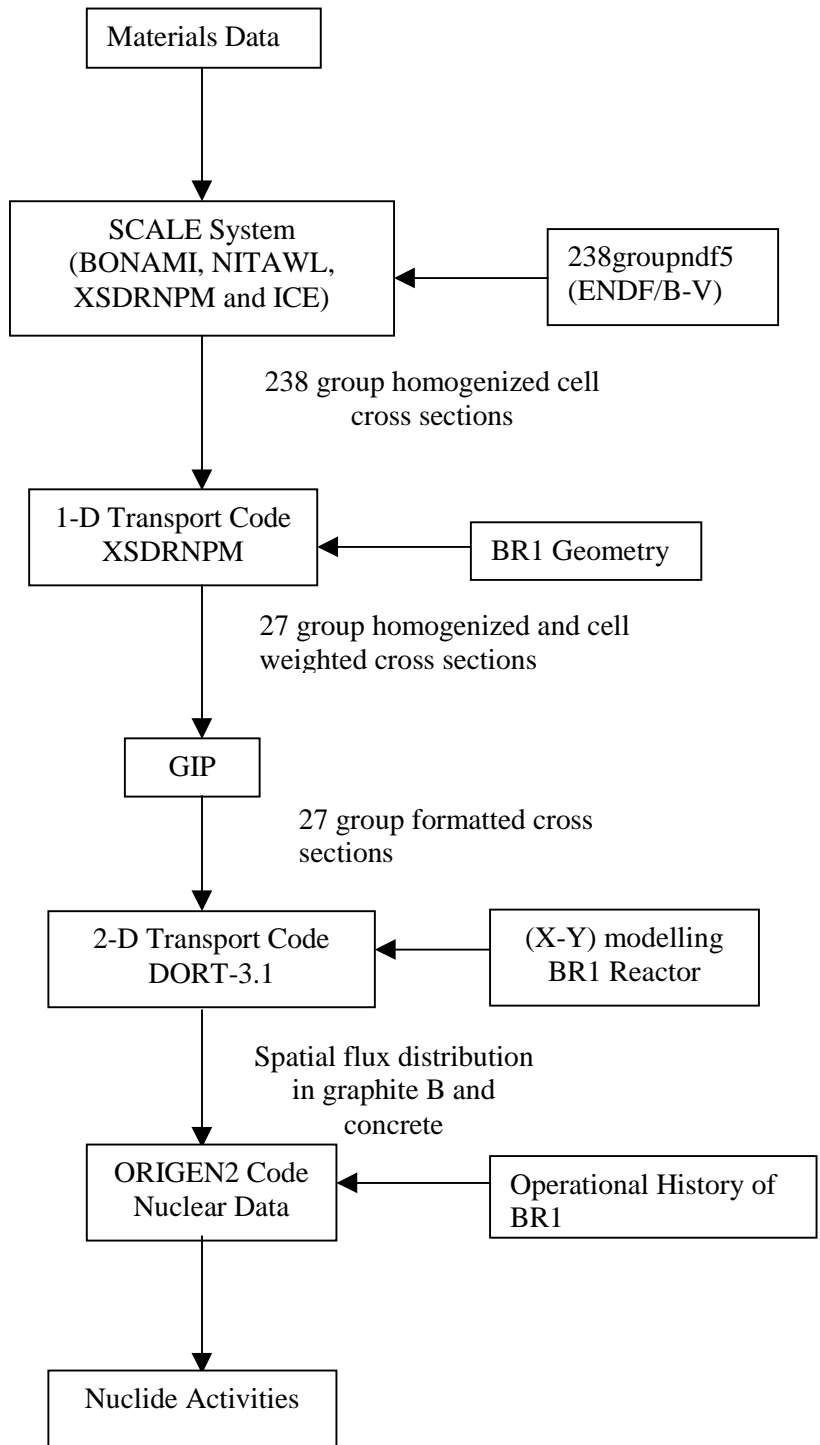


Figure 2. Flow chart of calculation scheme

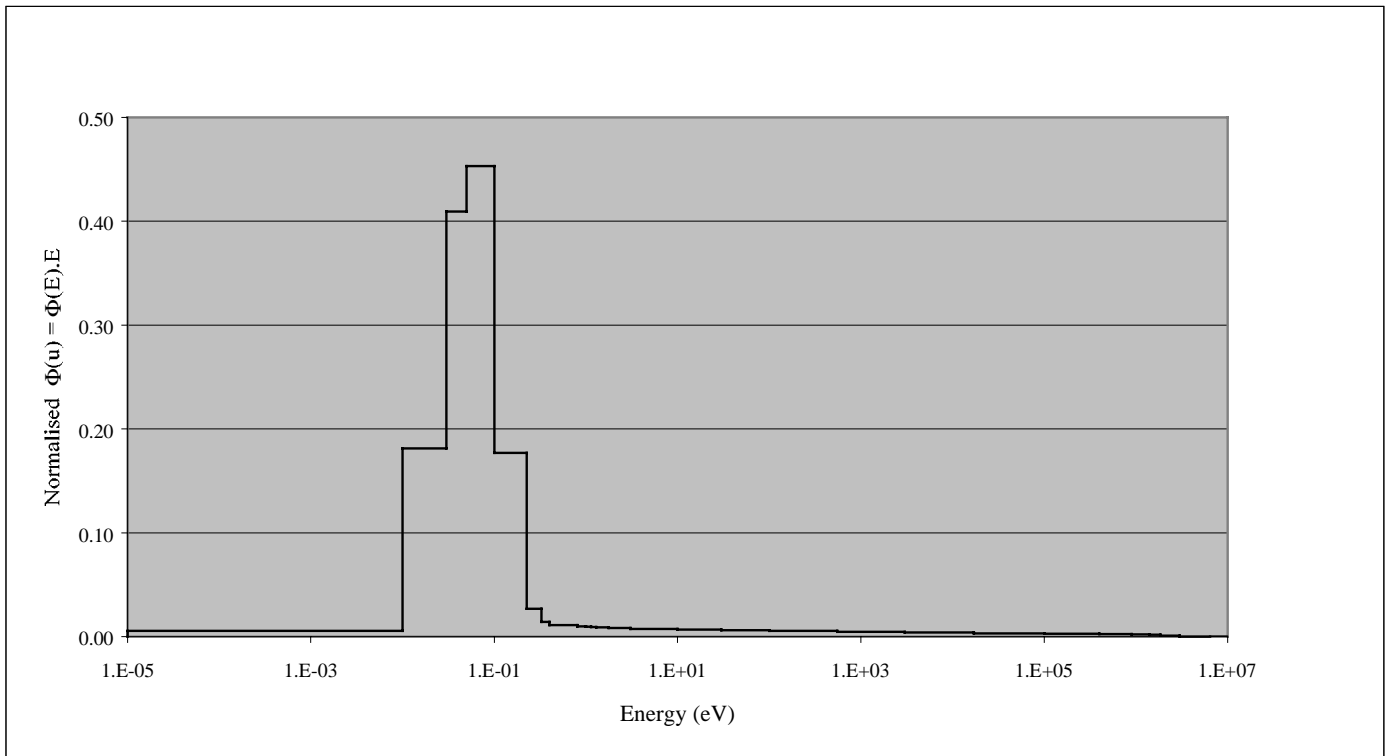


Figure 3. Energetic distribution of the neutron flux in Graphite B

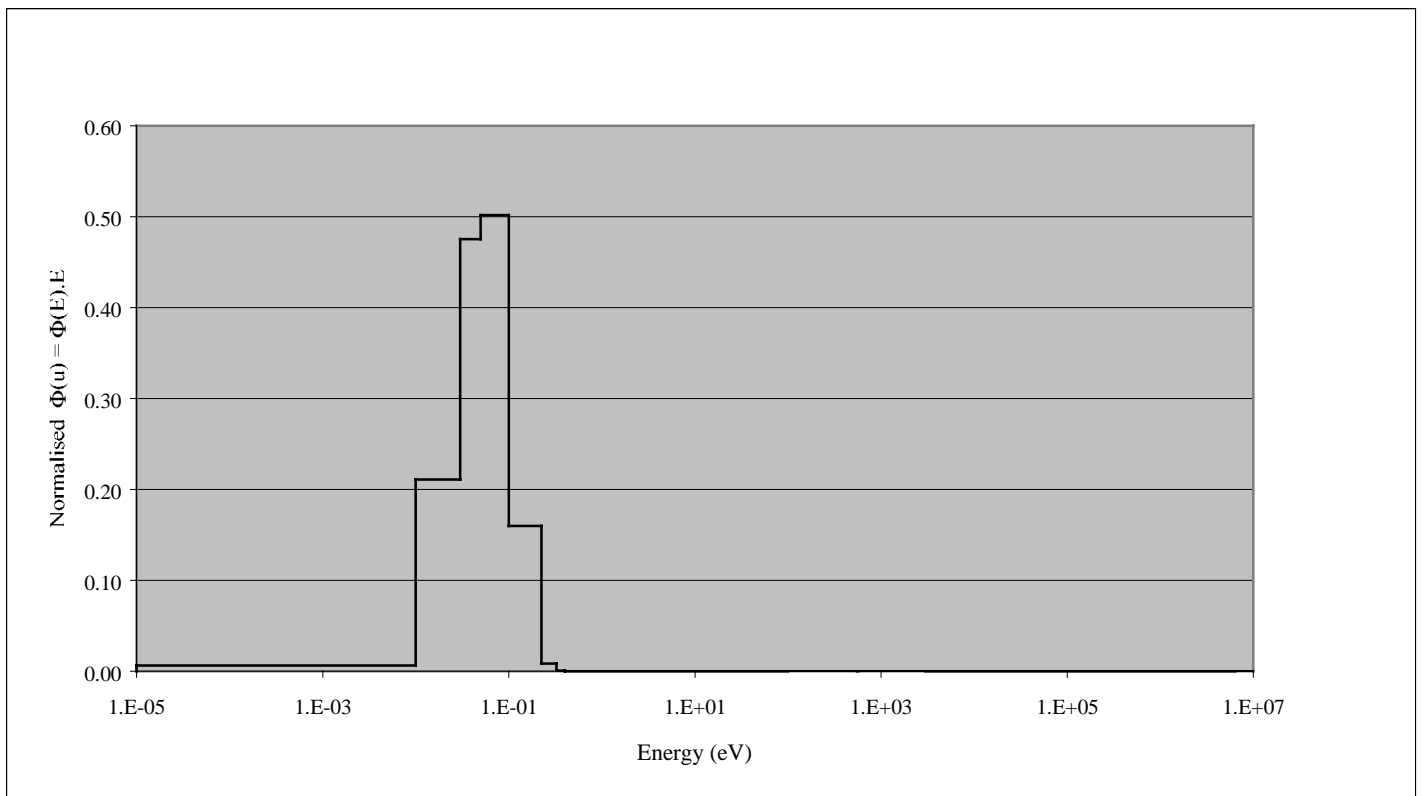


Figure 4. Energetic distribution of the neutron flux in Concrete

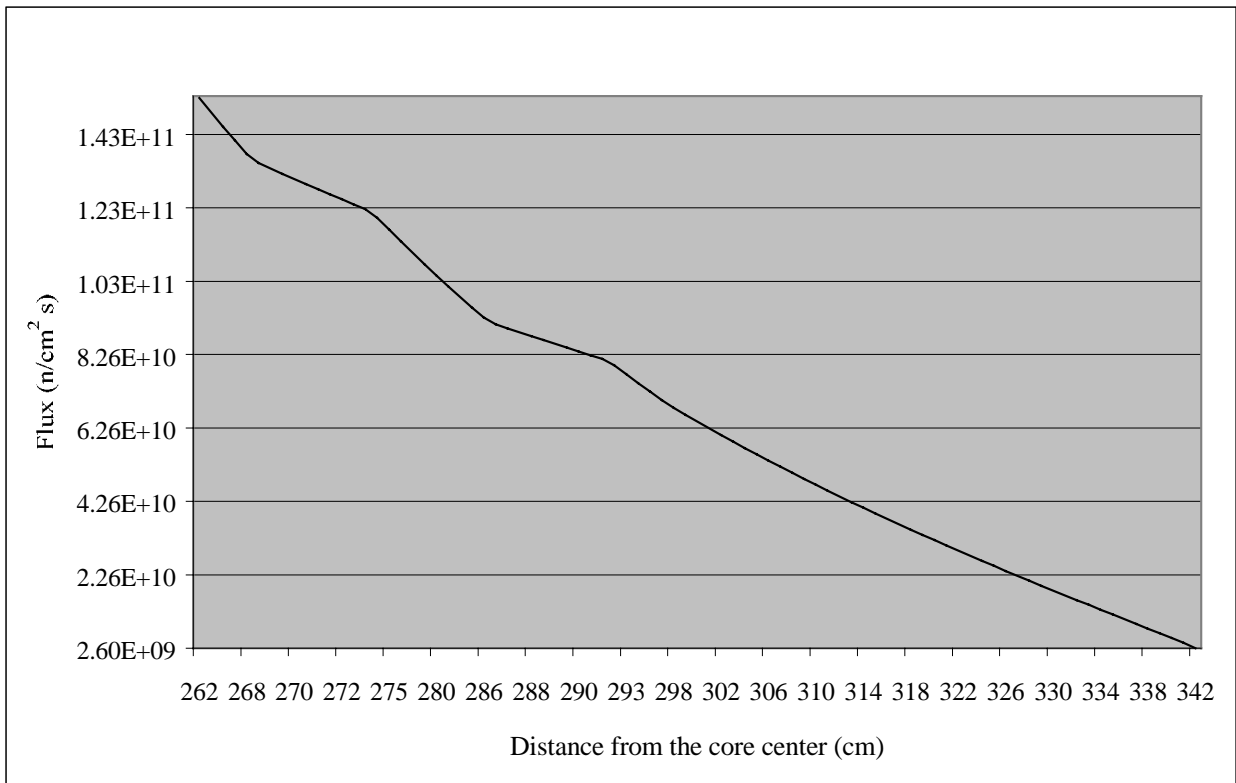


Figure 5. Flux depression in Graphite B

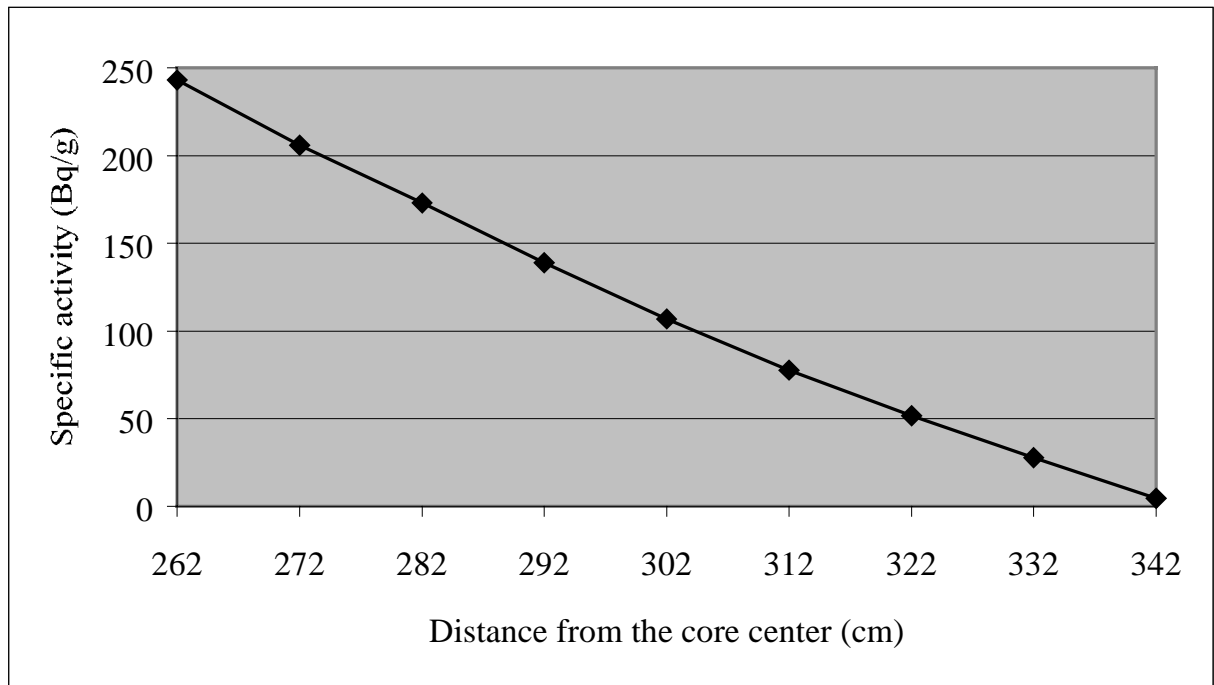


Figure 6. Specific activity depression in Graphite B

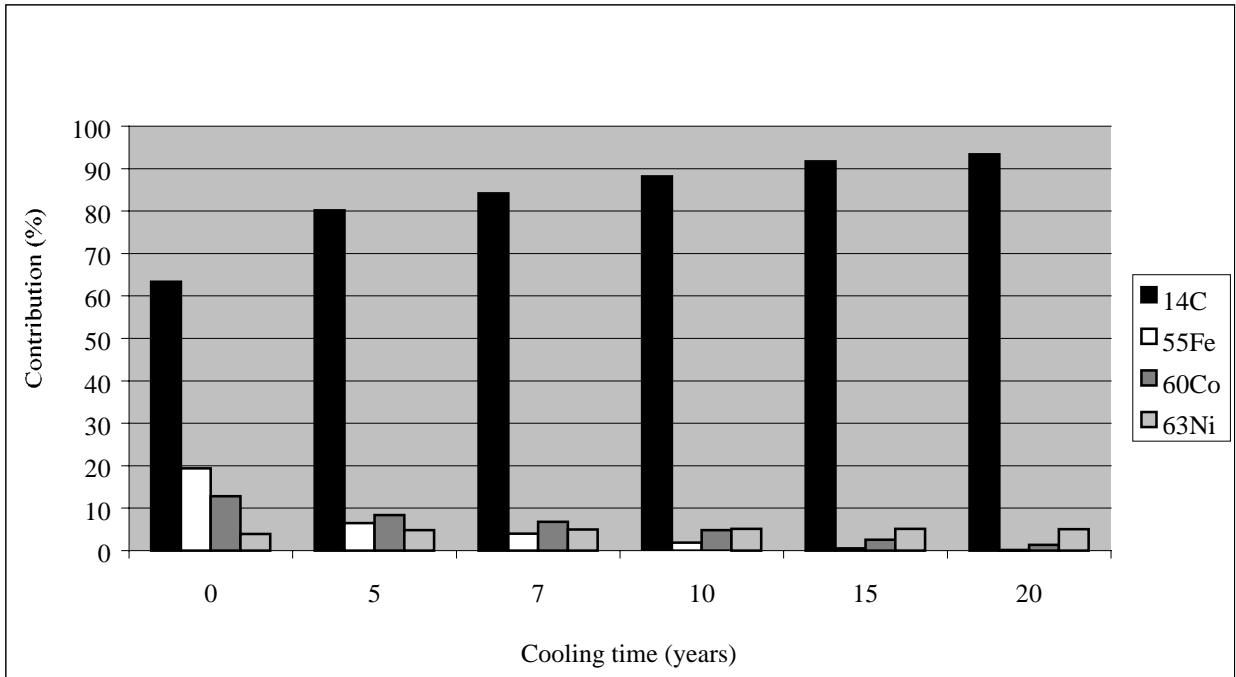


Figure 7. Isotope contributions to the specific activity in Graphite B with 0.01 ppm Co

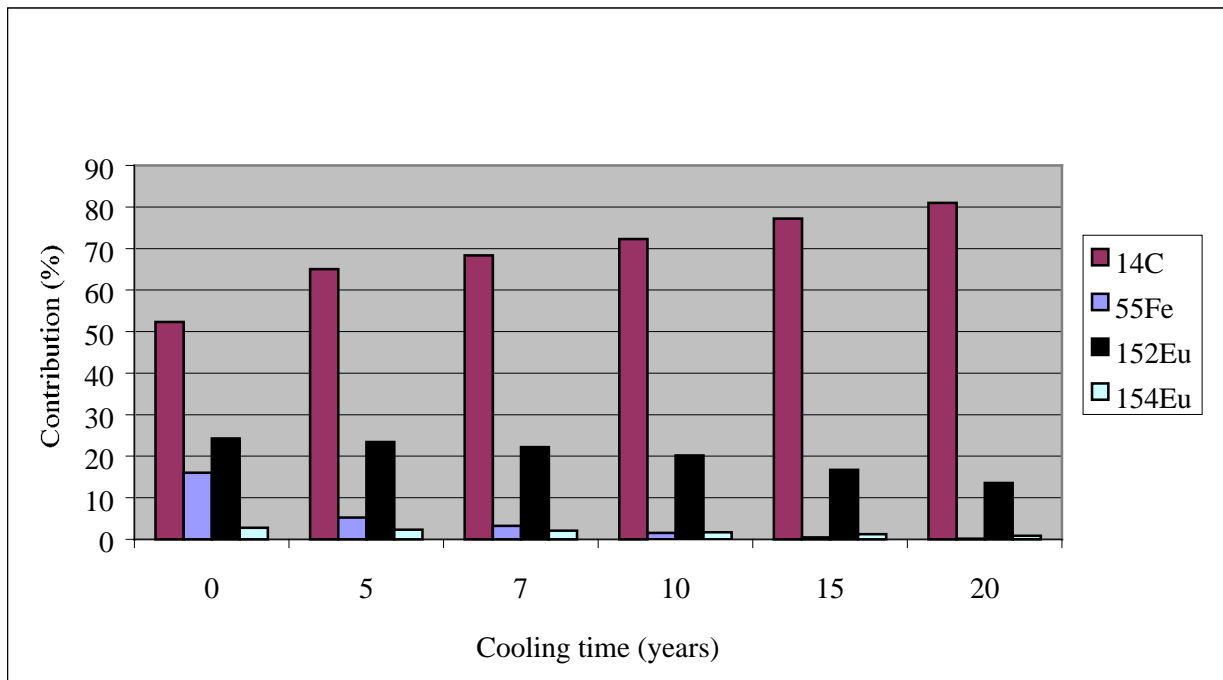


Figure 8. Isotope contributions to the specific activity in Graphite B with 0.001 ppm Eu

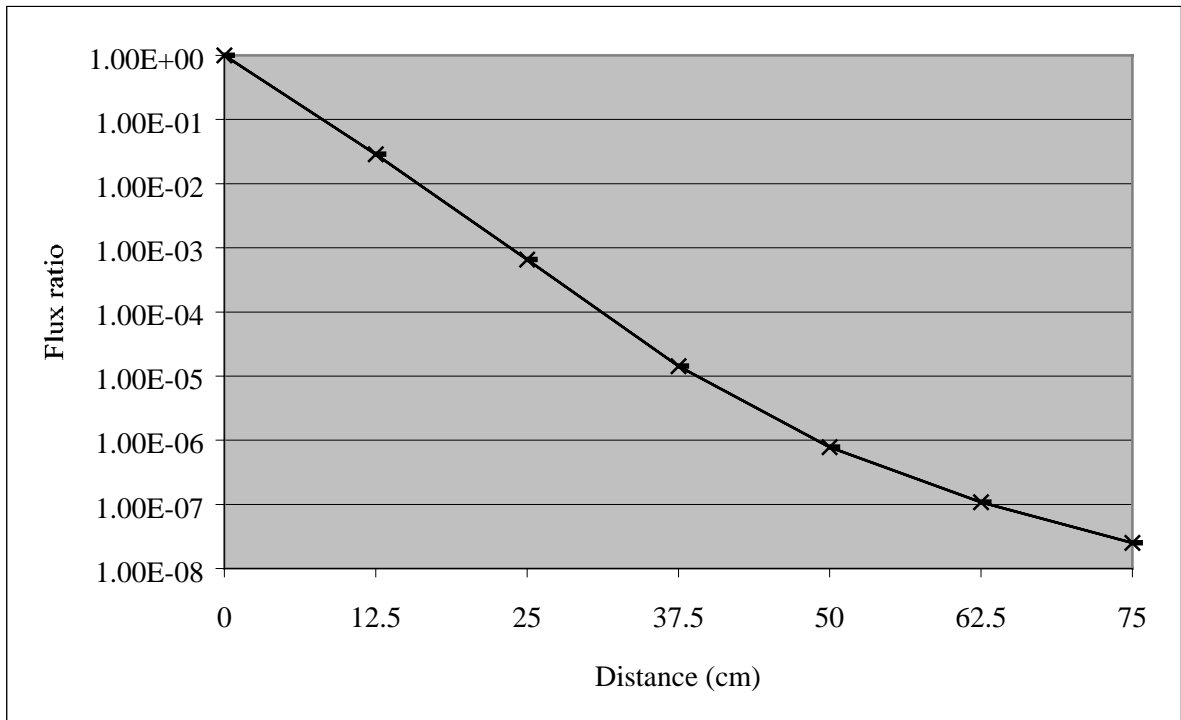


Figure 9. Flux depression in Concrete ( $\psi=45^\circ$ )

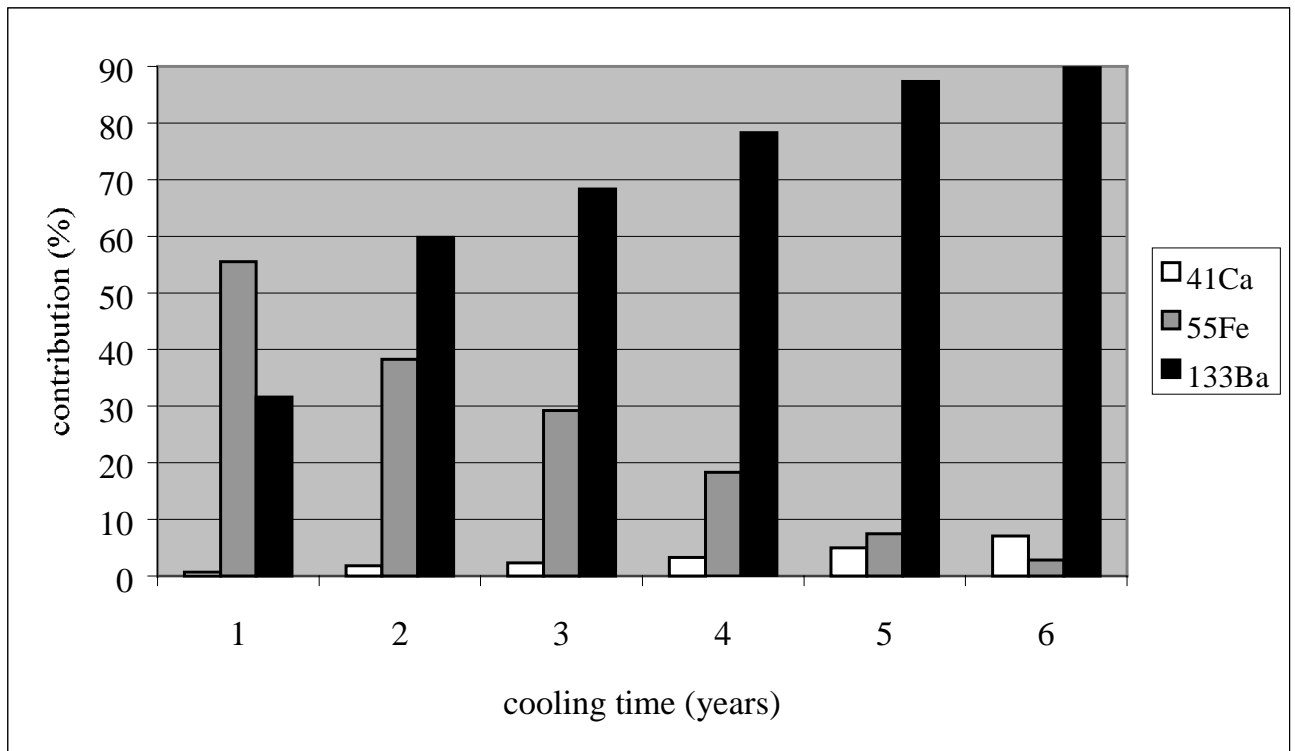


Figure 10. Isotope contributions to the activity in Concrete